Study of the local forces along a cutting edge when drilling Ti6Al4V – comparison of methods

Antoine Poutord, Frédéric Rossi and Gérard Poulachon*

Arts et Metiers ParisTech,
LaBoMaP, Rue porte de Paris 71250 Cluny, France
Email: antoine.poutord@yahoo.fr
Email: frederic.rossi@ensam.eu
Email: gerard.poulachon@ensam.eu
*Corresponding author

Rachid M'Saoubi

Seco Tools (UK) Ltd.,
Alcester, Warwickshire, UK
Email: rachid.msaoubi@secotools.com

Guillaume Abrivard

Airbus Group Innovations,
Centre Technocampus EMC2,
Chemin du Chaffault, 44340 Bouguenais, France
Email: guillaume.abrivard@airbus.com

Abstract: In aerospace applications, drilling is one of the most common operations. However, this machining stays complex and expensive, especially for difficult-to-cut materials such as titanium alloys. Because drilling is a blind operation, the physical measurements in-situ or the observation of phenomena close to the cutting edge is hard to observe. This study focuses on two different methods allowing the evaluation of the local forces along the main cutting edge. The first method is based on a physical decomposition of the drill edge. The global forces are measured when drilling samples with various external diameters: 1) smaller or larger than the drill diameter; 2) with or without pilot hole. The forces measurement for each sample lead to the determination of the elementary forces along the cutting edge and the margin. The second method decomposes the forces during the progressive drill point entry in the work material. On each Z level, the drill edge engagement is geometrically determined, allowing the knowledge of the elementary forces applied along the cutting edge and the margin.

Keywords: drilling; local forces; Ti6Al4V.

Reference to this paper should be made as follows: Poutord, A., Rossi, F., Poulachon, G., M'Saoubi, R. and Abrivard, G. (xxxx) 'Study of the local forces along a cutting edge when drilling Ti6Al4V – comparison of methods', *Int. J. Machining and Machinability of Materials*, Vol. X, No. Y, pp.xxx–xxx.

Biographical notes: Antoine Poutord is a young PhD who has defended his thesis at Arts et Metiers Paritech on 2014. He has mainly work during his research with Airbus and Seco Tools companies. The purpose of his scientific research was the challenge to drill a titanium/CFRP stack in one shot with the same drill. In this case, a new drill design has been defined with Seco Tools permitting to make industrially a large number of holes. Nowadays, he is Engineer-Doctor in an aerospace sub-contractor company in France.

Frédéric Rossi is an Associate Professor in the LaBoMaP at Arts et Métiers ParisTech (France). He studied mechanical engineering in this institution and defended his PhD in the field of metallurgical science working on alloys for nuclear applications. He has over nine years working experience in LaBoMaP, in the field of thermal modelling and experimentations developments, initially in the field of casting process and since 2010 in the field of machining.

Gérard Poulachon received his PhD in Manufacturing Engineering from Arts et Métiers ParisTech (France) in 1999. In 2006, he received his Habilitation to Manage Research (HDR) degree from the University of Lyon (France). Now, he is a full Professor at Arts et Metiers ParisTech and manages the research laboratory named LaBoMaP since 2012. He develops his main research activities on difficult-to-cut work materials, five axis machining, thermo mechanical modeling, and development of in-situ sensor in order to understand the mechanisms of chip formation. He has followed up to now 13 PhD students and published more than 40 papers in international journals. He is an associate member of the prestigious International Academy of Production Engineering (CIRP).

Rachid M'Saoubi received his PhD in Material Science and Engineering from Arts et Métiers ParisTech (France) in 1998. He joined the Swedish Institute for Metals Research in Stockholm in 1998 to conduct material research in cooperation with Swedish cutting tool manufacturers and steel companies. He is employed since 2006 as a Senior Scientist at Seco Tools in Sweden. His main research interest is the study of material behaviour in machining processes, the characterisation of wear mechanisms and surface integrity. He is a Fellow of the International Academy of Production Engineering (CIRP) and has published more than 40 papers in journals.

Guillaume Abrivard received his PhD in Materials Science from MINES ParisTech (France) in 2009. During his thesis, he developed a coupled crystal plasticity – phase field formulation to describe microstructural evolution during recrystallisation. In 2009, he joined the materials and processes team of Airbus Group Innovations, the corporate research Centre of Airbus group. His main research activity is focused on machining operations of aeronautic materials such as milling Ti alloys and drilling of composites/metallic assembly. He is also ensuring that new manufacturing technologies are mastered in collaboration with public labs and implemented into the various entities group.

1 Introduction

Aerospace industry uses more and more titanium alloys mainly for its high mechanical properties such as high strength-to-weight ratio, high resistance at elevated temperatures, and an elasticity modulus close to the carbon fibre reinforced plastic, enabling a good repartition of the stresses within the stack (Ezugwu and Wang, 1997; Ezugwu, 2005).

Drilling of Ti6Al4V alloy is a critical application because of the blind aspect operation combined with the low machinability of this material (Cantero, 2005). Most studies are focused on the global forces to understand the macroscopic cutting phenomena, the surface qualities (Dornfeld et al., 1999), and the thermo-mechanical modelling aspects (Ozcelik and Bagci, 2006). To increase the robustness of these models, the local forces along the cutting edge have to be known (Li and Shih, 2007a, 2007b).

Methods developed in the past to discretise the forces along the cutting edge could be presented in two mains categories.

- Method #1, based on a physical decomposition (Dargnat, 2006) is often used with various pilot holes and could be applied in different work materials, like bones (Lee et al., 2012), CFRP (Hamade et al., 2006) or titanium alloys (Bonnet, 2010).
- Method #2, developed more recently, is based on the decomposition of the forces during the drill point engagement in the work material (Claudin et al., 2008; Lazar and Xirouchakis, 2011, 2013).

These two methods are detailed in this paper by three particular experimentations in order to compare them.

Those experimental results can be compared to mechanistic models (Bissey, 2005; Campocasso et al., 2013; López de Lacalle et al., 2009; Sui et al., 2014; Parsian et al., 2014) or finite elements simulations (Abele and Fujara, 2010).

2 Experimental procedures

2.1 Tooling and equipment

Ti6Al4V β treated alloy samples are composed of 20 mm diameter rods machined in a 25 mm thickness plate. Drilling experiments were performed on two NC machines-tools. The first one is a two axis lathe (SOMAB Transmab 400) equipped with an 8,000 rpm spindle speed. The samples were gripped with an ER32 collet. The thrust force and the drilling torque were measured by a six components piezoelectric dynamometer Kistler 9121. The Z axis and spindle positions were acquired respectively by the 0.1 µm and 0.35° resolution optical coder. The second machine tool is a three axis DNC milling machine (DMC 65V) equipped with an 18,000 rpm spindle speed. Ti6Al4V specimens in this case were clamped directly on the milling table. The thrust force and torque were also measured by a six components piezoelectric dynamometer Kistler 9123. The Z axis position and spindle speed frequency were collected by the analogical output of the DNC (Siemens 840D) respectively with a 20 µm and 0.08 rpm resolution.

Table 1 Drill geometry

WC-Co drill (Grade K20)	
Drill diameter	12 mm
Flute length	55 mm
Point angle	140°
Helix angle	32°
Clearance angle (near outer diameter)	15°
Rake angle (near outer diameter)	32°
Back taper	0.5%
Margin width	0.8 mm

The signals were monitored by an A/D board (NI 9188 and three NI 9215 cards, National Instrument, USA, with a 50 kHz data acquisition frequency) and recorded on a PC using data acquisition software (Dasylab 11, NI, USA). The data were then operated with Matlab R2007b software.

A commercial drill (Seco-K20 type uncoated) recommended for titanium drilling was selected for this investigation. Main cutting tool parameters are listed in Table 1.

2.2 Experimental design

A previous study (Poutord et al., 2013) has permitted to select the suitable cutting parameters sets (Vc&f) (summarised in Table 2).

Table 2 Cutting conditions

WC Co drill (Grade K20)	
Work material	Ti6Al4V β
Cutting speed (Vc)	10 m/min
Spindle speed (N)	265 rpm
Feed (f)	0.2 mm/rev
Lubrication condition	Dry

A wear study of a drill selected in the same batch showed that the global cutting forces does not change significantly during the 18 firsts holes during Ti6Al4V drilling (Poutord et al., 2013). That point has been confirmed by a repetition of the first drilling test at the end of the experimental campaign.

2.2.1 Method #1: physical decomposition by varying the external diameter (discrete approach)

The first experiment used to subdivide the main drilling edge is based on a ‘physical decomposition’ as pointed out on Figure 2 and Table 4. Different edge portions of the drill are used during the drilling operation by varying the external diameters of the sample which could be prepared with or without a pilot hole as shown in Figure 1. The local forces are deduced by subtracting the global forces from neighbour trials. Table 3 presents the machining tests carried out in order to determine the local forces on seven sections of the edge drill. The pilot hole enables the physical subtraction of the chisel edge influence during the drilling operation.

Figure 1 Physical drill decomposition (see online version for colours)

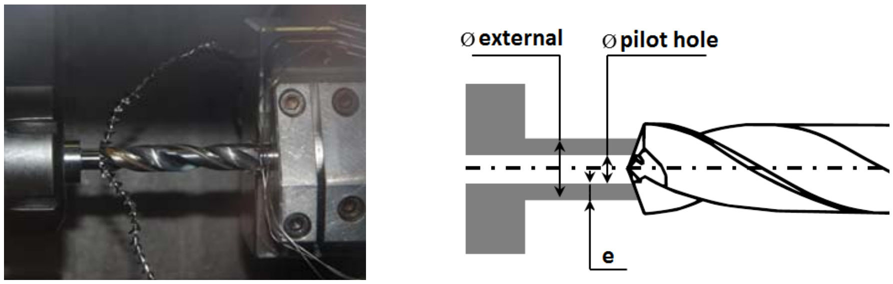

Table 3 Drilling experiments

Test #	*Pilot hole radius [mm]*	*External radius [mm]*	*e [mm]*
1	1.5	20	4.5
2	1.5	5.95	4.45
3	1.5	5.5	4
4	1.5	4.5	3
5	1.5	3.5	2
6	1.5	2.5	1
7	No pilot hole	20	6
8	No pilot hole	5.95	5.95
9	No pilot hole	5.5	5.5
10	No pilot hole	4.5	4.5
11	No pilot hole	3.5	3.5
12	No pilot hole	2.5	2.5

Table 4 Edge subdivision

Edge subdivision #	*Radius [mm]*
1	0–1.5
2	1.5–2.5
3	2.5–3.5
4	3.5–4.5
5	4.5–5.5
6	5.5-5.95
7	5.95–6 margin included

Figure 2 Edge subdivision

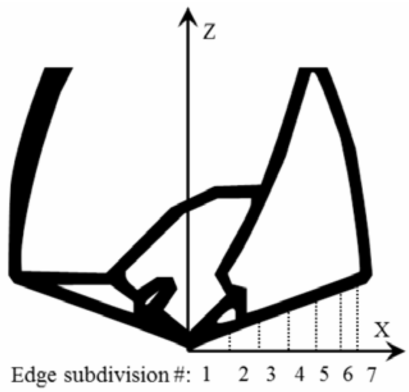

The procedure to calculate the global force on the chisel edge is based on the average of six values, as shown in equation (1):

$$F_{Calc_0}^{1.5} = \frac{1}{6} \cdot \sum \left(F_{Meas_0}^{k} - F_{Meas_{1.5}}^{k} \right) \quad k = [2.5; 3.5; 4.5; 5.5; 5.95; 10] \tag{1}$$

With, $F_{Calc_i}^{j}$ and $F_{Meas_i}^{j}$ which are respectively the force calculated and the force measured on an edge subdivision (*i* to *j*) of the drill radius.

The next edge segment from 1.5 mm to 2.5 mm on the radius is calculated by using the force calculated previously equation (2):

$$F_{Calc_{1.5}}^{2.5} = \frac{1}{2} \cdot \left(\left(F_{Meas_0}^{2.5} - F_{Meas_0}^{1.5} \right) + F_{Meas_{1.5}}^{2.5} \right) \tag{2}$$

The same methodology is used for the determination of the whole segments. Equation (3) presents the way to calculate the force applied on an edge segment *i* to *k* on the radius.

$$F_{Calc_i}^{k} = \frac{1}{4} \cdot \left(\left(F_{Meas_0}^{k} - F_{Meas_0}^{i} \right) + \left(F_{Mes_{1.5}}^{k} - F_{Mes_{1.5}}^{i} \right) + \left(F_{Mes_0}^{k} - F_{Calc_0}^{i} \right) + \left(F_{Mes_{1.5}}^{k} - F_{Calc_{1.5}}^{i} \right) \right) \tag{3}$$

The same calculi are used to determine the amount of the torque (T_z) applied on each segment of the edge. The local torque is then converted in the local cutting force (F_c) which is supposed to be constant on the entire edge segment [equation (4)].

$$Fc_i^k = T_{z_i}^k \cdot \frac{3 \cdot (k^2 - i^2)}{2 \cdot (k^3 - i^3)} \tag{4}$$

All the local forces are divided by the length of the segment in order to calculate the elementary force (except for the part of the edge near the margin). This allows the comparison between edge segments that have not the same length. The results are presented in the following section.

2.2.2 Method #1: physical decomposition by varying pilot hole diameter (discrete approach)

The previous way to discretise the edge was based on a reduction on the drilled diameter. In this experiment, the external radius drilled is always 12 mm, but the pilot holes are pre-drilled in order to reduce physically the contact length between the drill edge and the machined specimen.

Table 5 indicates the various radius of the pilot holes. Each configuration has been repeated three times in order to diminish the uncertainty on the measured values. Figure 3 presents the six different pilots holes performed for the edge decomposition.

This procedure permits to obtain practically similar lengths compared to the first experiment. The same kind of calculus is deployed to predict the elementary force in both cutting and thrust directions.

Table 5 Drilling experiments

Hole #	*Radius of the pilot hole [mm]*
1	No pilot hole
2	1.5
3	2.5
4	3.5
5	4.5
6	5.5
7	5.9

Figure 3 Plate of Ti6Al4V pre-drilled for the edge decomposition (see online version for colours)

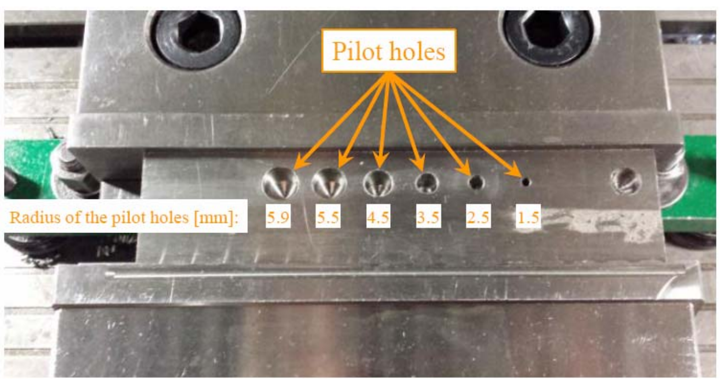

2.2.3 Method #2: point drill decomposition (continuous approach)

This method is based on the decomposition of the thrust force and the cutting torque during the progressive penetration of the drill point in the work material, so-called 'point drill discretisation'. With a precise determination of the point angle of the tool, the edge engagement can be deduced from the axial position of the tool as shown on Figure 4.

Figure 5 shows the variation of the thrust force and the cutting torque during the drilling of the Ti6Al4V workpiece. During the transient stage Figure 5(b), the edge is progressively engaged in the radial direction. As a result, the elementary force on the various sub-divisions is deduced by subtracting the effect of the previous sub-divisions.

To find the distribution along the main edge, the local torque is calculated in the same manner than the thrust force in order to determine the local tangential cutting forces. This cutting force is assumed to be constant on each edge segment and the application point of the equivalent local force located in the middle of each segment.

Figure 4 Link between the axial penetration and the drill edge engagement (see online version for colours)

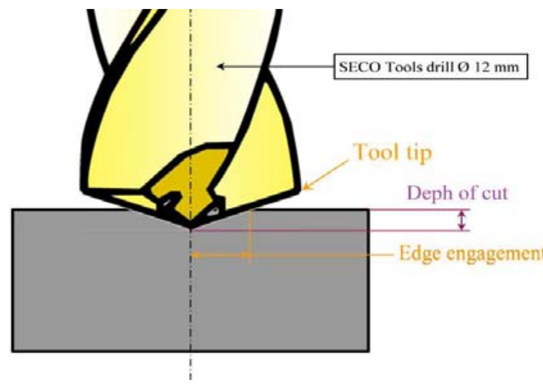

Figure 5 (a) Forces acquisition, (b) Zoom on the transient zone during the drilling of the test hole #7 (see online version for colours)

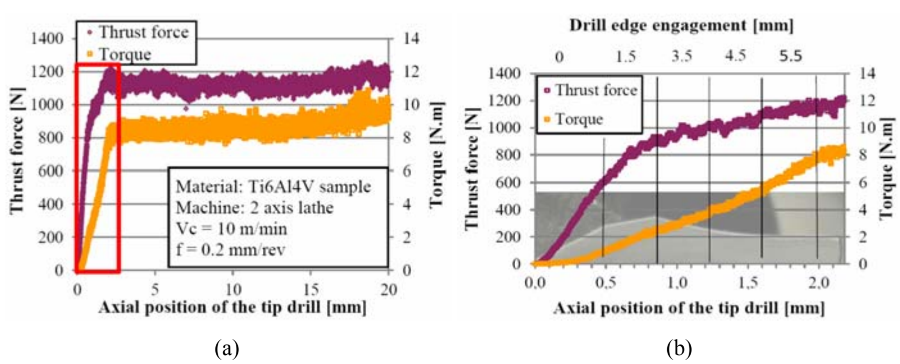

3 Results and discussion

3.1 Thrust force

The comparison between the three experiments concerning the thrust force is presented on Figure 6. The forces are indicated in (N/mm) to facilitate the comparison between each segment having various lengths.

The local forces distributions present a similar tendency whatever the methods used. However, the experiment 3 is easier to perform because there is no need to prepare specific specimens.

The force on the margin in experiment 1 is higher due to the low variation of the segment length situated in between (edge sub-division #7 Table 4) the tool tip and the margin. Thanks to the repetition, the calculated standard deviation is around 10–15 N/mm for the thrust force.

Each experiment shows that the chisel edge is the 'cutting' area where the elementary axial forces are the higher. Approximately 50% of the global thrust force is due to the chisel edge located from 0 to 1.5 mm radius. This decomposition points out the importance of the chisel edge design for a drilling operation. The tool tip and the margin are of prime importance as well. The experiments 2 and 3 highlight that the local thrust force could be negative on this edge area, tending to pull up the plate during the drilling operation.

Figure 6 Thrust force distribution along the cutting edge for the three experimentations (see online version for colours)

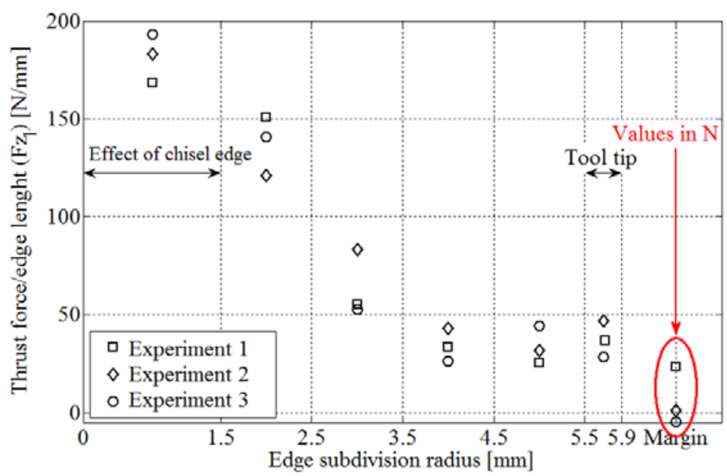

3.2 Cutting force

The approach used to compare the cutting forces is similar to the one used for the thrust force discussion (Section 3.1). Figure 7 presents the cutting forces by edge length (N/mm) in order to compare easily the various segments with different lengths.

Both local cutting forces distribution seems to present the same profile.

Each of the three experiments presents a quasi constant cutting force level all along the main cutting edge (≈ 150 N/mm). The level is twice as much high on the subdivisions situated between the web and 2.5 mm edge radius because the rake angle is almost null along the web edge area (Figure 8). Furthermore, the cutting speed is close to zero inducing high specific cutting forces. In consequence, a good design of the web thinning is important to limit the tool breakage.

If the tool tip and the margin show low forces level, the cutting speed and the amount of material removed by this part of the tool imply that the consumed power on that part of the tool is higher than on all the other parts of the tool.

That high level of energy on a little part implies heat elevation and tool failure risk. During wear tests on drilling, the part of the drill that breaks firstly is the tool tip, confirming the importance on the study of the power consumed by the cutting operation in function of the part of the edge to determine the critical part of the tool.

Figure 7 Cutting force along the edge for three methodologies (see online version for colours)

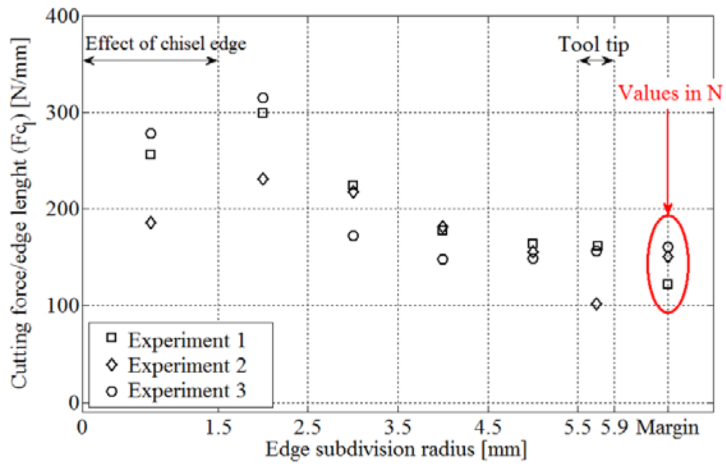

Figure 8 Tool angles along the edge of the drill (see online version for colours)

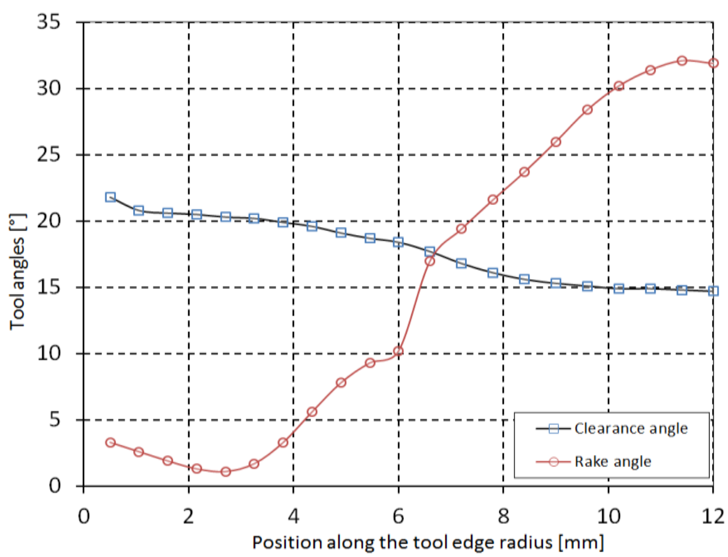

3.3 Sensitivity of the methods

Each analyse is based on the hypothesis of the segments independence. The only way to confirm that would be to collect the forces directly from a single edge part, like specific split tools (Kato et al., 1972; Barrow et al., 1982), that not seems to be possible for drills yet.

The physical decomposition (method #1), based on the discrete machining of multiple samples, implies a highly sensitivity to the tool wear and to the effective edge engagement. Each local force has to be calculated by various combinations of the global drilling forces in order to limit the errors. In turning (experiment 1), six combinations are used to calculate the influence of the drill web and four for each others areas. Moreover, the coaxiality between the tool and the sample needs to be precisely checked. In our case, the defect was inferior to 0.05 mm. During the pilot hole decomposition (experiment 2), few combinations are used, implying repetability tests to increase the precision of the model.

Method #2 is based on the numerical decomposition of the signals of the forces, implying a high sensitivity to the tool geometry, especially the point angle. In this study, the given point angle was 140°, whereas the measured one was 146.6°, associated to a drill point height of 1.8 mm. The numerical calculation must not shift the signals, and filtering the high frequency noise (the two frequencies with the most impacts appears one and two times a rotation).

4 Conclusions

If each method permits the evaluation of the local forces along the cutting edge, a few advantages and inconvenients are listed for each ones.

From an experimental point of view, the drill point decomposition method is easily carried out, the main constraint are the high velocity acquisition and the high sensitivity to the skin effect of the material (variation of the mechanical properties with the drilled depth engagement). The main advantage is that only one test is needed. The physical decomposition method is more difficult because many drilling operations are needed, also the influence of the drill wear.

The drill point decomposition needs a specific algorithm to treat the data; the starting point and the point angle have to be known precisely for a good reconstruction. The physical decomposition method has data that can be extracted easily.

The main advantage of the drill point decomposition method is the continuous aspect of this method. The length of the edge segments could be much more thin compare to the physical decomposition method; 0.1 mm length segments can be extracted with a good precision.

For the physical decomposition data, repeatability test for each diameter machined should be carried out to confirm the forces level for each parameter set. Some experiments allowing confirming the hypothesis done on the cutting forces part will be conducted.

Due to the proximity of the results, the point drill decomposition can be considered as the easier way to determine the forces along the cutting edge. This methodology based on single drilling opens perspectives on the determination of the bests cutting conditions to improve the precision of the tool material pair methodology (NF E 66 520). The other perspective can be linked with the drills design, allowing to determinate the most constrained part of the drill and the level of the forces on each part of it.

References

Abele, E. and Fujara, M. (2010) 'Simulation-based twist drill design and geometry optimization', *CIRP Annals – Manufacturing Technology*, Vol. 59, No. 1, pp.145–150.

Barrow, G., Graham, W., Kurimoto, T. and Leong, Y.F. (1982) 'Determination of rake face stress distribution in orthogonal machining', *International Journal of Machine Tool Design and Research*, Vol. 22, No. 1, pp.75–85.

Bissey, S. (2005) *Development of a Cutting Forces Model Applicable to a Family of Tools: Case of Milling of Hard Steels*, Arts et Metiers ParisTech, PhD dissertation, 184pp.

Bonnet, C. (2010) *Compréhension des mécanismes de coupe lors du perçage à sec de l'empilage Ti6Al4V Composite fibre de carbone*, PhD thesis, ENSAM Cluny, France.

Campocasso, S., Costes, J-P., Fromentin, G., Bissey-Breton, S. and Poulachon, G. (2013) 'Improvement of cutting forces modeling based on oriented cutting tests', *14th CIRP Conference on Modeling of Machining Operations*, Turin, Italy, No. 8, pp.206–211.

Cantero, J.L. (2005) 'Dry drilling of alloy Ti6Al4V', *International Journal of Machine Tools & Manufacture*, Vol. 45, No. 11, pp.1246–1255.

Claudin, C., Poulachon, G. and Lambertin, M. (2008) 'Correlation between drill geometry and mechanical forces in MQL conditions', in *Machining Science and Technology*, Vol. 12, No. 1, pp.133–144.

Dargnat, F. (2006) *Modélisation semi-analytique par approche énergétique du procédé de perçage de matériaux monolithiques*, PhD thesis, Université de Bordeaux I, No. 3216.

Dornfeld, D.A., Kim, J.S., Dechow, H., Hewson, J. and Chen, L.J. (1999) 'Drilling burr formation in titanium alloy, Ti-6AI-4V', *CIRP Annals – Manufacturing Technology*, Vol. 48, No. 1, pp.73–76.

Ezugwu, E.O. (2005) 'Key improvements in the machining of difficult-to-cut aerospace superalloys', *International Journal of Machine Tools & Manufacture*, Vol. 45, Nos. 12–13, pp.1353–1367.

Ezugwu, E.O. and Wang, Z.M. (1997) 'Titanium alloys and their machinability – a review', *Journal of Materials Processing Technology*, Vol. 68, No. 3, pp.262–274.

Hamade, R.F., Seif, C.Y. and Ismail, F. (2006) 'Extracting cutting force coefficients from drilling experiments, *International Journal of Machine Tools & Manufacture*, Vol. 46, Nos. 3–4, pp.387–396.

Kato, S., Yamaguchi, K. and Yamada, M. (1972) 'Stress distribution at the interface between tool and chip in machining', *Journal of Manufacturing Science and Engineering*, Vol. 94, No. 12, pp.683–689.

Lazar, M-B. and Xirouchakis, P. (2011) 'Experimental analysis of drilling fiber reinforced composites', *International Journal of Machine Tools & Manufacture*, Vol. 51, No. 12, pp.937–946.

Lazar, M-B. and Xirouchakis, P. (2013) 'Mechanical load distribution along the main cutting edges in drilling', *Journal of Materials Processing Technology*, Vol. 213, No. 2, pp.245–260.

Lee, J.E., Gozen, B.A. and Ozdoganla, O.B. (2012) 'Modeling and experimentation of bone drilling forces', *Journal of Biomechanics*, Vol. 45, No. 6, pp.1076–1083.

Li, R. and Shih, A.J. (2007a) 'Spiral point drill temperature and stress in high-throughput drilling of titanium', *International Journal of Machine Tools & Manufacture*, Vol. 47, Nos. 12–13, pp.2005–2017.

Li, R. and Shih, A.J. (2007b) 'Tool temperature in titanium drilling', *Transaction of ASME*, Vol. 129, No. 4, pp.740–749.

López de Lacalle, L.N., Rivero, A. and Lamikiz, A. (2009) 'Mechanistic model for drills with double point-angle edges', *The International Journal of Advanced Manufacturing Technology*, Vol. 40, Nos. 5–6, pp.447–457.

Ozcelik, B. and Bagci, E. (2006) 'Experimental and numerical studies on the determination of twist drill temperature in dry drilling – a new approach', *Materials & Design*, Vol. 27, No. 10, pp.920–927.

Parsian, A., Magnevall, M., Beno, T. and Eynian, M. (2014) 'A mechanistic approach to model cutting forces in drilling with indexable inserts', *Procedia CIRP*, Vol. 24, pp.74–79.

Poutord, A., Rossi, F., Poulachon, G., M'Saoubi, R. and Abrivard, G. (2013) 'Local approach of the wear in drilling Ti6Al4V/CFRP for stack modeling', *Procedia CIRP*, Vol. 8, pp.316–321.

Sui, J., Sugita, N., Ishii, K., Harada, K. and Mitsuishi, M. (2014) 'Mechanistic modeling of bone-drilling process with experimental validation', *Journal of Materials Processing Technology*, Vol. 214, No. 4, pp.1018–1026.